APPLIED AND ENVIRONMENTAL MICROBIOLOGY, Nov. 2003, p. 6644–6649 Vol. 69, No. 11
0099-2240/03/$08.00+0 DOI: 10.1128/AEM.69.11.6644–6649.2003

Diffusional Properties of Methanogenic Granular Sludge: ^{1}H NMR Characterization

Piet N. L. Lens,[1,2]* Rakel Gastesi,[2,3] Frank Vergeldt,[1] Adriaan C. van Aelst,[4] Antonio G. Pisabarro,[3] and Henk Van As[1]

Laboratory of Biophysics,[1] Subdepartment of Environmental Technology,[2] and Plant Cell Biology,[4] University of Wageningen, 6700 EV Wageningen, The Netherlands, and Department of Agrarian Production, Public University of Navarra, Pamplona, Spain[3]

Received 6 March 2002/Accepted 17 August 2003

The diffusive properties of anaerobic methanogenic and sulfidogenic aggregates present in wastewater treatment bioreactors were studied using diffusion analysis by relaxation time-separated pulsed-field gradient nuclear magnetic resonance (NMR) spectroscopy and NMR imaging. NMR spectroscopy measurements were performed at 22°C with 10 ml of granular sludge at a magnetic field strength of 0.5 T (20 MHz resonance frequency for protons). Self-diffusion coefficients of H_2O in the investigated series of mesophilic aggregates were found to be 51 to 78% lower than the self-diffusion coefficient of free water. Interestingly, self-diffusion coefficients of H_2O were independent of the aggregate size for the size fractions investigated. Diffusional transport occurred faster in aggregates growing under nutrient-rich conditions (e.g., the bottom of a reactor) or at high (55°C) temperatures than in aggregates cultivated in nutrient-poor conditions or at low (10°C) temperatures. Exposure of aggregates to 2.5% glutaraldehyde or heat (70 or 90°C for 30 min) modified the diffusional transport up to 20%. In contrast, deactivation of aggregates by $HgCl_2$ did not affect the H_2O self-diffusion coefficient in aggregates. Analysis of NMR images of a single aggregate shows that methanogenic aggregates possess a spin-spin relaxation time and self-diffusion coefficient distribution, which are due to both physical (porosity) and chemical (metal sulfide precipitates) factors.

Nuclear magnetic resonance (NMR) is a powerful technique for studying cellular tissues (17). NMR spectroscopy of ^{1}H, ^{13}C, and ^{31}P nuclei allows determination of the chemical composition of a cellular tissue, from which metabolic pathways can be deduced. The anatomy of a tissue can be visualized by NMR imaging, which is mostly based on differences in magnetic relaxation rates within the cellular tissue. The best-known examples of NMR tissue studies come from medical applications, but NMR has also been used in studies of cellular assemblies of mammalian, plant, and bacterial cells.

NMR studies of biofilms and bioreactors have thus far received only little attention, despite their huge potential for the study of transport processes, i.e., self-diffusion and flow, in these systems (18, 32). The major attractions of NMR are that it is noninvasive, so that no biomass deactivation is needed, it is independent of the transparency of the biofilm, and the measurement is not disturbed by the presence of inorganic inclusions or sand particles. Thus, NMR methods overcome the disadvantages of many conventional methods for measuring diffusion coefficients, which are mostly done ex situ (in a measuring or flow cell) on selected (geometry) and deactivated aggregates (20). Another special property of NMR is that flow can be detected in any direction within the sample, in contrast to X-ray, optical, and ultrasound scattering flow methods, which measure only a net flow between the emitter and the detector.

* Corresponding author. Mailing address: Subdepartment of Environmental Technology, University of Wageningen, Bomenweg 2, P.O. Box 8129, 6700 EV Wageningen, The Netherlands. Phone: 31 317 483851. Fax: 31 317 484208. E-mail: piet.lens@wur.nl.

The most widely applied method of studying transport processes in bioreactors is pulsed-field gradient (PFG) NMR (27), which has been used for detailed studies of water transport processes in pipes and model systems (3), polystyrene beads (28, 29), and soils (33). In addition to quantifying ^{1}H displacement, PFG NMR also discriminates different ^{1}H pools in a tissue, which correspond to different physical and chemical environments (12), on the basis of the longitudinal and/or transverse relaxation times.

PFG NMR has been applied to study the diffusional characteristics of methanogenic granular sludge (2, 14, 16). Methanogenic granular sludge consists of rigid, well-settling microbial aggregates that develop by the mutual attachment of bacterial cells in the absence of a carrier material (19). As in biofilms and cellular tissues, molecular diffusion is the predominant mass transport process of soluble substrate molecules in methanogenic aggregates (20). Beuling et al. (2) validated the PFG NMR analysis using a series of artificial aggregates of different densities and loaded with different bacterial cell concentrations. They showed that the apparent diffusion coefficient of granular sludge determined by PFG NMR analysis agreed well with those obtained with glucose microelectrodes. Lens et al. (16) analyzed in detail the PFG NMR data obtained with one type of aggregate growing on pulp and paper mill wastewater. They found that the aggregates contain a distribution of self-diffusion coefficients, varying between 1.0×10^{-9} $m^2 s^{-1}$ (bacterial-cell-associated water) and 2.1×10^{-9} $m^2 s^{-1}$ (matrix-associated water).

This paper reports an analysis using PFG NMR of the diffusional properties of different types of granular sludge grown under different operational conditions in laboratory and full-

TABLE 1. Processing conditions of the bioreactors where the different types of anaerobic aggregates used in this study were cultivated

Reactor location or aggregate type	Wastewater type	Reactor configuration	Operational temp (°C)	Reference
Full-scale reactors				
Industriewater (Eerbeek, The Netherlands)	Pulp and paper	UASB	30	16
Heineken (Zoeterwoude, The Netherlands)	Brewery	EGSB	30	6
Grolsh (Enschede, The Netherlands)	Brewery	UASB	30	
Cargill (Sas van Gent, The Netherlands)	Food	UASB	30	
Archer Daniels Midland (Ringaskiddy, Ireland)	Citric acid	UASB	30	
Laboratory-scale reactors				
Thermophilic	Oleate	EGSB	55	8
Psychrophilic	Malting wastewater	Two-stage UASB	10	23
Sulfidogenic I	Volatile fatty acids[a]	USSB	30	15
Sulfidogenic II	Volatile fatty acids[a]	Baffled	30	31

[a] Chemical oxygen demand/sulfate ratio, 0.5.

scale reactors. In addition, the effect of deactivation methods commonly used to determine the diffusional properties of biofilms was investigated. Finally, PFG NMR imaging was used to study the spatial resolution of the transverse relaxation time (T_2) and self-diffusion within individual aggregates.

MATERIALS AND METHODS

Source of biomass. Different types of methanogenic and sulfidogenic granular sludge were harvested from full- and laboratory-scale anaerobic granular sludge reactors (Table 1). The operational conditions and aggregate characteristics of most of these reactors have been described previously (Table 1).

Aggregate preparation and treatment. After anaerobic sampling of the aggregates, fine particles were elutriated with anaerobic tap water. Aggregates were used without pretreatment for the NMR measurements, unless indicated otherwise. To determine the effect of the aggregate size on the diffusional properties, the aggregates were sieved with metallic sieves (DIN 4188; Retsch, Haan, Germany) in order to obtain the different size fractions. Aggregates were deactivated by submerging them in a 2.5% (vol/vol) glutaraldehyde or 0.2% (vol/vol) $HgCl_2$ solution for 3.5 and 2.5 h, respectively. For heat treatment, aggregates were submerged in hot water for 0.5 h at either 70 or 97°C.

NMR measurements. All NMR measurements were done at room temperature (22 ± 1°C) on a 0.47 T (20.35 MHz) imager consisting of a Surrey Medical Imaging Systems (Guildford, United Kingdom) console, a Bruker electromagnet (Karlsruhe, Germany), and a probe head (Doty Scientific Inc., Columbia, S.C.) with active shielded gradients (35, 36). A probe with a cylindrical sample space with an inner diameter of 3.0 cm was used for the T_2 and diffusion measurements. All NMR measurements were performed in a glass tube (inner diameter, 2.5 cm) containing 10 ml of methanogenic unfed (degassed) granular sludge.

Self-diffusion coefficient measurements. Self-diffusion coefficients were determined using diffusion analysis by relaxation time separated (DARTS) PFG NMR, as described by van Dusschoten et al. (35). Typical acquisition parameters were as follows: repetition time, 6 s (four averages); spectral width, 100 kHz, number of echoes, 2,000, with an echo time of 1.05 ms. The gradient pulses were given after two dummy scans of 10 s each and had a duration of 5 ms; the observation time was 12.1 ms (unless specified otherwise), during which three 180° radiofrequency pulses were given with an interval (2*TAU dif) of 2.9 ms. The data set obtained with the self-diffusion measurement was analyzed by using nonlinear least-squares fitting routines (35).

NMR imaging. Functional imaging and data processing to simultaneously obtain the amplitude, T_2, and self-diffusion coefficient were done with a PFG-Carr Purcell Meiboom Gill sequence as described by van Dusschoten et al. (35). Typical acquisition parameters were as follows: repetition time, 1 s (four averages); spectral width, 50 kHz; number of echoes, 64, with an echo time of 5 ms. The field of view was 10 mm, with a slice thickness of 2 mm, yielding 128 × 128 voxels with a resolution of 80 × 80 × 2,000 μm^3. The gradient pulses had a duration of 2.5 ms; the observation time was 10 ms, during which three 180° radio frequency pulses were given with an interval of 3.1 ms. To calibrate the density of the aggregates within the image, agar beads (1 and 10%, wt/vol) prepared as described by Beuling et al. (2) were included in the same image.

Microscopy. Granular sludge anatomy was investigated with a Leica (Rijswijk, The Netherlands) MZ8 stereomicroscope as described by Alphenaar et al. (1). Normal and back-scattering scanning electron microscopy (SEM) was done at, respectively, 8 and 15 keV on intact and cleaved (with a razor blade) aggregates after dehydration with a gradient series of ethanol and critical-point drying by using a JEOL 5200 SEM as described by Gonzalez-Gil et al. (6).

RESULTS

Self-diffusion coefficient of methanogenic granular sludge. Tables 2 and 3 show that the diffusional properties of methanogenic aggregates strongly depend on their origin. The self-

TABLE 2. Effect of aggregate size on the self-diffusion coefficient, T_2 and D/D_{aq} of different methanogenic aggregates sampled from mesophilic full-scale anaerobic UASB bioreactors and a thermophilic laboratory-scale reactor

Wastewater type and size fraction (diam [mm])	D^a (10^{-9} m^2/s)	T_2 (ms)	D/D_{aq} (%)
Pulp and paper (Eerbeek)			
0.5–1.0	1.36 ± 0.02	49.3	63
1.0–1.4	1.22 ± 0.03	46.3	56
>1.4	1.39 ± 0.01	42.0	64
Brewery I (Heineken)			
0.5–1.0	1.20 ± 0.02	49.3	67
1.0–1.4	1.16 ± 0.01	46.3	68
1.4–2.0	1.16 ± 0.03	30.0	65
>2.0	1.27 ± 0.01	46.8	74
Brewery II (Grolsh)			
0.5–1.0	1.31 ± 0.03	50.4	77
1.0–1.4	1.34 ± 0.02	44.7	77
>1.4	1.26 ± 0.03	28.9	76
Food (Cargill)			
1.0–1.4	1.32 ± 0.01	49.3	69
1.4–2.0	1.29 ± 0.03	45.7	78
>2.0	1.29 ± 0.03	47.1	78
Citric acid (Ringaskiddy), all fractions	1.32 ± 0.02	45.3	61
Thermophilic oleate-degrading aggregates, all fractions	1.68 ± 0.03	25.7	86

[a] Values are means ± standard deviations from triplicate experiments.

TABLE 3. Effect of deactivation procedures on the T_2 and D/D_{aq} ratio of methanogenic aggregates

Sample type	D^a (10^{-9} m^2/s)	T_2 (ms)	D/D_{aq} (%)
Pulp and paper wastewater (Eerbeek)[b]			
Intact	1.39 ± 0.01	42.0	64
Deactivated with:			
Glutaraldehyde	1.14 ± 0.01	27.0	52
$HgCl_2$	1.39 ± 0.02	45.0	64
Heat (70°C)	1.88 ± 0.04	58.8	87
Heat (97°C)	1.99 ± 0.03	78.9	92
Citric acid (Ringaskiddy)			
Intact	1.32 ± 0.02	45.3	61
Deactivated with:			
Glutaraldehyde	1.08 ± 0.03	22.0	47
$HgCl_2$	1.34 ± 0.01	43.5	62
Heat (70°C)	1.54 ± 0.02	65.7	71
Heat (97°C)	1.77 ± 0.03	73.5	82

[a] Values are means ± standard deviations from triplicate experiments.
[b] Measurements using the sludge fraction with a diameter of >1.4 mm.

TABLE 4. Effect of process operation on the self-diffusion coefficient of water in anaerobic aggregates

Reactor type	D^a (10^{-9} m^2/s)	T_2 (ms)	D/D_{aq} (%)
Psychrophilic acidifying reactor[b]			
Stage I			
Top	1.11 ± 0.01	37	51
Middle	1.28 ± 0.02	43	59
Bottom	1.42 ± 0.01	49	65
Stage II			
Top	1.11 ± 0.01	20	51
Middle	1.12 ± 0.03	32	51
Bottom	1.25 ± 0.01	34	58
Sulfidogenic volatile fatty acid-degrading reactors			
Inoculum	1.59 ± 0.01	11	73
UASB[c]	1.58 ± 0.01	7	73
USSB[c]			
Compartment 1	1.72 ± 0.02	4	79
Compartment 2	1.61 ± 0.01	7	74
Compartment 3	1.54 ± 0.02	6	71
Compartment 4	1.51 ± 0.05	5	69
Compartment 5	1.67 ± 0.01	6	76
Baffled reactor[d]			
Compartment 1	1.51 ± 0.03	8	69
Compartment 2	1.52 ± 0.09	6	70
Compartment 3	1.49 ± 0.08	8	68

[a] Values are means ± standard deviations from triplicate experiments.
[b] Aggregates were sampled after 161 days of reactor operation.
[c] Aggregates were sampled after 138 days of reactor operation.
[d] Aggregates were sampled after 91 days of reactor operation. The inoculum was the sulfidogenic UASB sludge.

diffusion coefficient of H_2O in mesophilic aggregates varied between 1.22×10^{-9} m^2 s^{-1} (pulp and paper reactor) and 1.34×10^{-9} m^2 s^{-1} (brewery II reactor), corresponding to 56 and 77% of the self-diffusion coefficient of free water, respectively. Aggregates grown at a low temperature (10°C) also had a low self-diffusion coefficient of H_2O (Table 4), varying between 1.11×10^{-9} and 1.42×10^{-9} m^2 s^{-1}, corresponding to, respectively, 51 and 65% of the H_2O self-diffusion coefficient of free water. In contrast, thermophilic aggregates showed a fast diffusional transport (Table 2), as shown by a self-diffusion coefficient only 14% lower than that of free water.

Effect of the aggregate size. Table 2 shows that the self-diffusion coefficient of mesophilic methanogenic aggregates was independent of the investigated size fractions.

Effect of deactivation of methanogenic aggregates. Table 3 shows that deactivation of methanogenic aggregates strongly alters their diffusional transport behavior. Glutaraldehyde reduces the self-diffusion of H_2O by 20%, whereas heat exposure strongly increases (20 to 35% at 70°C) the self-diffusion coefficient of H_2O within methanogenic aggregates (Table 3). Deactivation by $HgCl_2$ did not alter the self-diffusion coefficient compared to untreated aggregates (Table 3).

Effect of reactor design and reactor operation. Table 4 shows that the self-diffusion coefficient of H_2O is higher in the aggregates present at the bottom of a sludge bed, where substrate- and nutrient (influent wastewater)-rich conditions prevail, than in the aggregates present at the top of a sludge bed, where lower substrate concentrations prevail. Table 4 further shows that the segregation of granular sludge beds into compartments with different metabolic activities also leads to aggregates with different diffusional properties, as evidenced by the different self-diffusion coefficients of H_2O of aggregates cultivated in the sulfidogenic upflow anaerobic sludge bed (UASB) and upflow staged sludge bed (USSB) reactors, which developed out of the same inoculum. However, the operation time also plays an important role, as cultivation of granular sludge in a baffled reactor over a short (3-month) period hardly affected the self-diffusion coefficient of H_2O within these aggregates (Table 4).

Spatial distribution of diffusion coefficients in individual aggregates. The anatomy of a single methanogenic thermophilic aggregate with a heterogeneous structure, i.e., containing concentric biomass layers as well as cavities (Fig. 1A), was investigated by nuclear magnetic imaging. The T_2 image of the aggregate shows a T_2 distribution and thus confirms that H_2O is present in different physical environments within a single aggregate (Fig. 1C). Back-scattering electron microscopy images (Fig. 1B), which reflect the metal distribution of the sample, show that metal precipitates, e.g., FeS, are abundant in the core of the aggregate, but they are also randomly distributed in small spots within the aggregate. High-resolution SEM observations showed that metal precipitates are located around microbial, most likely *Methanosaeta* sp., cells (data not shown).

Figure 2 shows a nuclear magnetic image of the amplitude, T_2, and the self-diffusion coefficient of the thermophilic methanogenic aggregate shown in Fig. 1A. To compare it with defined solid matrixes, beads made of 1 and 10% (wt/vol) agar were also positioned in the magnet in separate test tubes. Figure 2 clearly confirms the heterogeneous physical structure of the aggregate, as indicated by the distribution of T_2 (Fig. 2B)

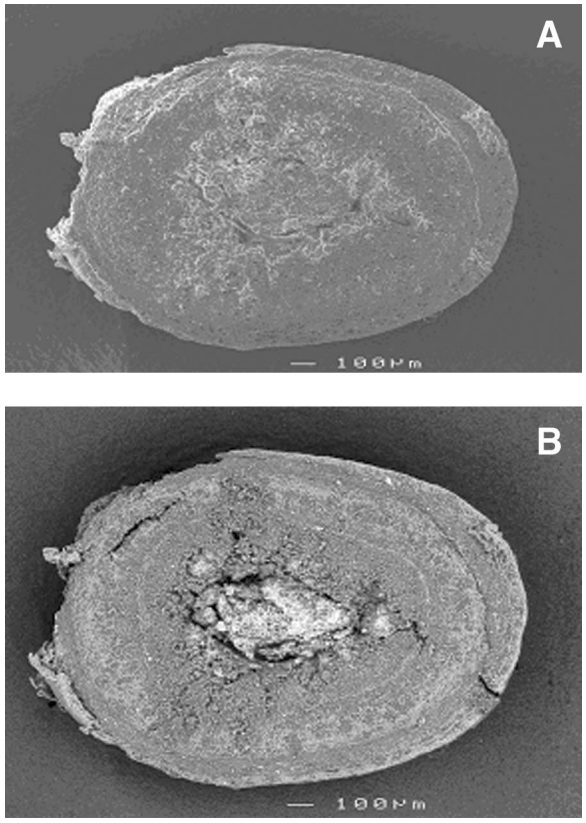

FIG. 1. Structure of a thermophilic (55°C) methanogenic aggregate treating oleate wastewater. Low-magnification electron-microscopic images of the aggregate shown in Fig. 2, cleaved upon termination of the NMR image, are presented. (A) Normal scanning electron microscopy. (B) Back-scattering electron microscopy. Dark areas in the back-scattered electron image indicate regions with higher biomass concentrations, whereas light areas indicate regions with high metal content. (C) Map of the spin-spin relaxation rate (R_2; $1/T_2$) of a test tube containing a five intact thermophilic aggregates immersed in demineralized water and a reference tube filled with $MnCl_2$-doped demineralized water (central tube). The spatial resolution of this T_2 map is 80 μm, and the slice thickness is 2 mm. White areas indicate regions with a high R_2, whereas dark areas indicate regions with a low R_2. Note that R_2 is the result of the physicochemical environment, i.e., pore size, polymer density, or metal sulfide precipitates (32).

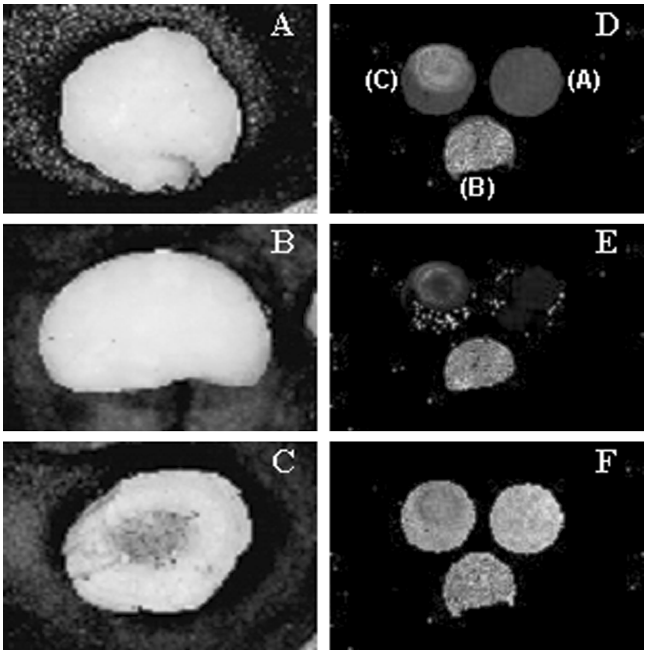

FIG. 2. NMR images of the spatial variation of ^{1}H NMR parameters in a slice of 2 mm of an insert containing a single methanogenic aggregate (Fig. 1A). (A to C) Low-magnification light-microscopic images of cross-sectioned beads: 1% agar (A), 10% agar (B), and methanogenic aggregate (C). (D to F) NMR images: amplitude (D), R_2 (= $1/T_2$) (E), and self-diffusion coefficient (F). Letters in panel D indicate the different beads.

and the self-diffusion coefficient (Fig. 2C) within a single aggregate.

DISCUSSION

Heterogeneity of diffusional transport in methanogenic aggregates. This study shows that the NMR protocols used to study transport processes in porous media can also be applied to bacterial aggregates containing large amounts of paramagnetic inclusions, e.g., FeS (Fig. 1B). The latter are known to cause severe line broadening at high magnetic field strengths (12), thus excluding this type of system from NMR investigations at high field strengths. However, the use of low magnetic field strengths, e.g., 0.5 T, as applied in this study, enables successful application of PFG NMR in methanogenic aggregates.

Figures 1 and 2 confirm that methanogenic aggregates contain T_2 distributions, as was also found for the pulp and paper (16) and brewery I aggregates (6). These distributions are typical for porous media and have been reported for inert materials, i.e., rocks, concrete, and agarose gels, as well as for biological tissues, i.e., mushrooms and plant leaves (25). As in these other microporous systems, ^{1}H relaxation of water in methanogenic granular sludge is multiexponential (data not shown) and much faster than that of bulk water (Tables 2 to 4). Both physical (pore size distribution) (Fig. 1C) and chemical (distribution of metal precipitates) (data not shown) factors contribute to the T_2 decay (11).

The self-diffusion image (Fig. 2) confirms that methanogenic

granular sludge contains a self-diffusion coefficient distribution, as reported previously for different types of aggregates (6, 16). The distribution of the diffusion coefficient can be of biological, instrumental, or statistical origin. Evidence for the biological nature of the scatter in self-diffusion coefficients in microporous membranes has been demonstrated by Monte Carlo simulations (24). Experimental evidence has been given for diffusion coefficient distributions of flat aerobic biofilms, using microslicing techniques (39), miniaturized limiting current techniques (38), and microinjection of fluorescent dyes in combination with confocal microscopy (4). All these studies showed that the diffusion coefficient distribution could be related to gradients in biofilm density and porosity. This study shows that this is also the case for methanogenic granular sludge, as the self-diffusion coefficient distribution corresponds to the T_2 distribution (Fig. 2), which is directly related to the porosity or density of the granular sludge matrix (10).

Effect of operational parameters on diffusion coefficients of granular sludges. In contrast to nuclear magnetic imaging, the NMR spectroscopic results (Tables 2 to 4) give no information on the spatial distribution of the self-diffusion values. Beuling et al. (2) showed that a monoexponential analysis of the ^{1}H NMR diffusion data set, also applied in this work, gives an accurate estimate of the apparent diffusion coefficient of organic substrates in aggregates. The ratios of the self-diffusion coefficient in the aggregate to that of free water (D/D_{aq}) (56 to 78%) (Tables 2 and 3) are in the same range as those reported for aerobic biofilms (20, 22, 26) and for other methanogenic aggregates (1, 13).

High substrate concentrations, such as those prevailing at the bottom of UASB reactors, induce the formation of looser aerobic biofilms (22) and methanogenic aggregates (Table 4), with a faster diffusional transport. Similarly, growth of aggregates at elevated (55°C) temperatures also leads to the development of looser aggregates, with fast diffusional transport (Table 2). Figure 1 shows that these aggregates also contain cavities, which can develop because of the high decay rates under thermophilic conditions or during starvation periods (1). In contrast, growth of aggregates at low temperatures (10°C) results in the formation of dense and compact aggregates with a slow diffusional transport (Table 4), as has also been reported for immobilized nitrifying microorganisms (37).

Exposure of biofilms to glutaraldehyde or heat to eliminate microbial activity is widely applied in diffusion coefficient measurement protocols (20). Table 3 shows that these procedures strongly affect the diffusional transport in the aggregate matrix. The strongly protein-oxidizing action of glutaraldehyde considerably reduces the H_2O self-diffusion in the methanogenic aggregates. In contrast, exposure to heat makes the matrix more permeable, as evidenced by the increase in self-diffusion coefficient (Table 2). This confirms the work of Tatevossian (30) and Lens et al. (13), who also found that glutaraldehyde and heat treatment significantly affects the transport properties of cell aggregates. In agreement with results reported by Matson and Characklis (21), deactivation of microbial metabolism by $HgCl_2$ did not alter the self-diffusion coefficient compared to that in untreated aggregates. Thus, $HgCl_2$ deactivation of aggregates can be recommended for measurement techniques of the diffusion coefficient that rely on biomass deactivation.

Applicability of NMR to anaerobic aggregates. In addition to diffusive substrate transport, convective transport has been proposed to contribute to mass transport in methanogenic granular sludge (7). Convective transport in aggregates has been correlated with the presence of higher upflow velocities (6 to 10 m h^{-1}) of the reactor liquid in expanded granular sludge bed (EGSB) reactors (9) or with pressure oscillations (about 1 atm) on aggregates looping in water columns as high as 20 m in internal circulation reactors (34). Applying pressure oscillations of 1 atm of overpressure to acetate-fed granular sludge during the DARTS PFG NMR diffusion measurements did not allow unequivocal demonstration the presence of convective transport (data not shown). Detection and quantification of this type of mass transport by NMR warrant further research with q-space NMR procedures (29).

The diffusion data presented in this study relate to ^{1}H of water, which was used as the tracer molecule. NMR procedures are, however, not restricted to ^{1}H of water. The self-diffusion coefficients of the ^{1}H of specific organic molecules, e.g., glucose or volatile fatty acids, can be determined by chemical shift imaging (27) or double quantum editing techniques (5). These techniques depress the signal of the extremely abundant water molecules (about 55 M) in order to visualize protons of organic compounds usually present in the micromolar or millimolar range. Alternatively, other nuclei can be used as tracers, as for example the use of ^{19}F NMR to probe directly the self-diffusion coefficient of fluorinated organic molecules (e.g., ^{19}F-glucose).

ACKNOWLEDGMENTS

We thank D. van Dusschoten for help with the diffusion coefficient measurements.

This research was supported by a TMR Marie Curie fellowship (ERBFMBICT950250) and the Human Capital and Mobility EU Large Scale Facility, Wageningen NMR Centre (ERBCHGECT940061).

REFERENCES

1. **Alphenaar, P. A., M. C. Perez, and G. Lettinga.** 1993. The influence of substrate transport limitation on porosity and methanogenic activity of anaerobic sludge granules. Appl. Microbiol. Biotechnol. **39:**276–280.
2. **Beuling, E. E., D. van Dusschoten, P. Lens, J. C. van den Heuvel, H. van As, and S. P. P. Ottengraf.** 1998. Characterization of the diffusive properties of biofilms using pulsed field gradient nuclear magnetic resonance. Biotechnol. Bioeng. **60:**283–291.
3. **Caprihan, A., and E. Fukushima.** 1990. Flow measurements by NMR. Phys. Rep. **198:**195–235.
4. **de Beer, D., P. Stoodley, and Z. Lewandowski.** 1997. Measurement of local diffusion coefficients in biofilms by microinjection and confocal microscopy. Biotechnol. Bioeng. **53:**151–158.
5. **de Graaf, R. A.** 1998. *In vivo* NMR spectroscopy. Principles and techniques. John Wiley, New York, N.Y.
6. **Gonzalez-Gil, G., P. Lens, A. Van Aelst, H. Van As, A. I. Versprille, and G. Lettinga.** 2001. Cluster structure of anaerobic aggregates of an expanded granular sludge bed reactor. Appl. Environ. Microbiol. **67:**3683–3692.
7. **Huisman, J. W., J. C. Van den Heuvel, and S. P. P. Ottengraf.** 1990. Enhancement of external mass transfer by gaseous end products. Biotechnol. Prog. **6:**425–429.
8. **Hwu, C.-S., and G. Lettinga.** 1997. Acute toxicity of oleate to acetate-utilizing methanogens in mesophilic and thermophilic anaerobic sludges. Enzyme Microb. Technol. **21:**297–301.
9. **Kato, M. T., J. A. Field, P. Versteeg, and G. Lettinga.** 1994. Feasibility of expanded granular sludge bed reactors for the anaerobic treatment of low strength soluble wastewater. Biotechnol. Bioeng. **44:**469–479.
10. **Kleinberg, R. L.** 1994. Pore size distributions, pore coupling, and transverse relaxation spectra of porous rocks. Magn. Reson. Imaging **12:**271–274.
11. **Le Bihan, D.** 1991. Molecular diffusion nuclear magnetic resonance imaging. Magn. Reson. Q. **17:**1–30.
12. **Le Bihan, D.** 1995. Molecular diffusion, tissue microdynamics and microstructure. NMR Biomed. **8:**375–386.

13. **Lens, P., D. de Beer, C. Cronenberg, F. Houwen, S. Ottengraf, and W. Verstraete.** 1993. Heterogeneous distribution of microbial activity in methanogenic aggregates: pH and glucose microprofiles. Appl. Environ. Microbiol. **59:**3803–3815.
14. **Lens, P., L. W. Hulshoff Pol, G. Lettinga, and H. Van As.** 1997. Use of ^{1}H NMR to study transport processes in sulfidogenic granular sludge. Water Sci. Technol. **36:**157–163.
15. **Lens, P., M. van den Bosch, L. W. Hulshoff Pol, and G. Lettinga.** 1998. Effect of staging on volatile fatty acid degradation in a sulfidogenic granular sludge reactor. Water Res. **32:**1178–1192.
16. **Lens, P., F. Vergeldt, G. Lettinga, and H. van As.** 1999. ^{1}H-NMR study of the diffusional properties of methanogenic aggregates. Water Sci. Technol. **39:** 187–194.
17. **Lens, P. N. L., and M. A. Hemminga.** 1998. Nuclear magnetic resonance in environmental engineering: principles and applications. Biodegradation **9:**393–409.
18. **Lens, P. N. L., and H. Van As.** 2003. Use of ^{1}H NMR to study transport processes in biofilms, p 285–307. *In* P. Lens, T. Mahony, T. Moran, P. Stoodley, and V. O'Flaherty (ed.), Biofilms in medicine, industry and environmental biotechnology: analysis, composition and control. International Water Association, London, United Kingdom.
19. **Lettinga, G.** 1995. Anaerobic digestion and wastewater treatment systems. Antonie Leeuwenhoek **67:**3–28.
20. **Libicki, S. B., P. M. Salmon, and C. R. Robertson.** 1988. The effective diffusive permeability of a nonreacting solute in microbial cell aggregates. Biotechnol. Bioeng. **32:**68–85.
21. **Matson, J. V., and W. G. Characklis.** 1976. Diffusion into microbial aggregates. Water Res. **10:**877–885.
22. **Onuma, M., T. Omura, T. Umita, and J. Aizawa.** 1985. Diffusion coefficient and its dependency on some biochemical factors. Biotechnol. Bioeng. **27:** 1533–1539.
23. **Rebac, S., S. Gerbens, P. Lens, J. B. van Lier, A. J. M. Stams, K. J. Keesman, and G. Lettinga.** 1999. Kinetics of fatty acid degradation by psychrophilically grown anaerobic granular sludge. Bioresource Technol. **69:**241–248.
24. **Saxton, M. J.** 1997. Single-particle tracking: the distribution of diffusion coefficients. Biophys. J. **72:**1744–1753.
25. **Schaafsma, T. J., H. Van As, W. D. Palstra, J. E. M. Snaar, and P. A. de Jager.** 1992. Quantitative measurement and imaging of transport processes in plants and porous media by ^{1}H NMR. Magn. Reson. Imaging **10:**827–836.
26. **Stewart, P. S.** 1998. A review of experimental measurements of effective diffusive permeabilities and effective diffusion coefficients in biofilms. Biotechnol. Bioeng. **59:**261–272.
27. **Stilbs, P.** 1987. Fourier transform pulsed-gradient spin-echo studies of molecular diffusion. Prog. Nuclear Magn. Reson. Spectrosc. **19:**1–45.
28. **Tallarek, U., K. Albert, E. Bayer, and G. Guiochon.** 1996. Measurement of transverse and axial apparent dispersion coefficients in packed beds. AIChE J. **42:**3041–3054.
29. **Tallarek, U., D. van Dusschoten, H. Van As, G. Guiochon, and E. Bayer.** 1998. Direct observation of fluid mass transfer resistance in porous media by NMR spectroscopy. Angew. Chem. Int. Ed. **37:**1882–1885.
30. **Tatevossian, A.** 1985. Some factors affecting the diffusion of [^{14}C]-lactate in human dental plaque. Arch. Oral Biol. **30:**141–146.
31. **Vallero, M., P. Lens, L. W. Hulshoff Pol, and G. Lettings.** 2003. Sulfidogenic volatile fatty acid degradation in a baffled reactor. Water Sci. Technol. **488:**81–88.
32. **Van As, H., and P. N. L. Lens.** 2001. Use of ^{1}H NMR to measure transport processes in porous biosystems. J. Ind. Microbiol. Biotechnol. **26:**43–52.
33. **Van As, H., and D. van Dusschoten.** 1997. NMR methods for imaging of transport processes in micro-porous systems. Geoderma **80:**389–403.
34. **Van den Heuvel, J. C., I. Portegies Zwart, and L. H. J. Vredenbregt.** 1996. Convective acceleration of mass transfer in three-phase systems by pressure oscillations. Chem. Eng. Sci. **51:**2391–2398.
35. **van Dusschoten, D., P. A. De Jager, and H. Van As.** 1995. Extracting diffusion constants from echo-time-dependent PFG NMR data using relaxation-time information. J. Magn. Reson. Ser. A **116:**22–28.
36. **van Dusschoten, D., P. A. De Jager, and H. Van As.** 1995. Flexible PFG NMR desensitized for susceptibility artifacts, using the PFG multiple-spin-echo sequence. J. Magn. Reson. Ser. A **112:**237–240.
37. **Wijffels, R. H., G. Englund, J. H. Hunik, E. J. T. M. Leenen, A. Bakketun, A. Gunther, J. M. Obon de Castro, and J. Tamper.** 1995. Effects of diffusion limitation on immobilized nitrifying microorganisms at low temperatures. Biotechnol. Bioeng. **45:**1–9.
38. **Yang, S., and Z. Lewandowski.** 1995. Measurement of local mass transfer coefficient in biofilms. Biotechnol. Bioeng. **48:**737–744.
39. **Zhang, T. C., Y.-C. Fu, and P. L. Bishop.** 1995. Competition for substrate and space in biofilms. Water Environ. Res. **67:**992–1003.